

# CT Versus Sonography for Monitoring Radiofrequency Ablation in a Porcine Liver

Charles H. Cha<sup>1</sup>  
Fred T. Lee, Jr.<sup>2</sup>  
Jonathan M. Gurney<sup>2</sup>  
Brian K. Markhardt<sup>2</sup>  
Thomas F. Warner<sup>3</sup>  
Frederick Kelcz<sup>2</sup>  
David M. Mahvi<sup>1</sup>

**OBJECTIVE.** The objective of this study was to compare CT and sonography for monitoring radiofrequency (RF) lesions in porcine livers.

**SUBJECTS AND METHODS.** RF lesions ( $n = 12$ ) were created in three pig livers by applying 13 min of current to a multielectrode RF probe with a target temperature of 95°C. Helical unenhanced CT and corresponding axial sonography were performed before ablation, at 2 min, 8 min, and immediately after ablation. Contrast-enhanced CT was performed after ablation. CT scans and sonograms were evaluated by blinded observers for conspicuity of the RF lesion, edge detection (visibility of liver-lesion interface), and artifacts. Hounsfield units were recorded at every time interval, and radiologic-pathologic correlation for lesion size and configuration was performed.

**RESULTS.** Mean size of RF lesions was  $3.03 \pm 0.9$  cm. On CT, RF lesions had consistently lower attenuation values than surrounding liver (22.2 H lower than liver at 8 min,  $p < 0.0001$ ). Echogenicity was variable with sonography (hypoechoic = 59%, hyperechoic = 25%, isoechoic = 16%). Unenhanced CT significantly improved conspicuity, edge detection of RF lesions, and decreased artifacts compared with sonography ( $p < 0.05$ ). Contrast-enhanced CT improved RF lesion detection, border discrimination, and artifacts compared with sonography ( $p < 0.05$ ). Unenhanced CT had the best correlation to pathologic size ( $r = 0.74$ ), followed by contrast-enhanced CT ( $r = 0.72$ ) and sonography ( $r = 0.56$ ). Contrast-enhanced CT best correlated with lesion shape, but slightly overestimated size because of areas of ischemia peripheral to the RF lesion.

**CONCLUSION.** In this animal model, unenhanced CT was an effective way to monitor RF ablation compared with sonography because of increased lesion discrimination, reproducible decreased attenuation during ablation, and improved correlation to pathologic size.

**P** rimary liver neoplasms and metastatic disease of the liver represent a significant source of morbidity and mortality in the United States. Hepatocellular carcinoma is one of the most common cancers in the world, with an annual incidence of at least 1 million new patients [1]. Approximately 150,000 new cases of colon cancer are diagnosed each year in the United States, of which approximately 50% will have recurrences within the first 5 years. Of these recurrences, 20% are predominantly localized to the liver [2]. The survival rate for untreated patients with of both these diseases is dismal. Surgical resection remains the gold standard in the treatment of hepatic tumors and more recently, cryoablation has been shown to confer a survival advantage in the absence of systemic disease [3–8]. Unfortunately, only approximately 10–20% of

patients with either primary or metastatic liver disease are amenable to surgical therapy [2]. In addition, patients technically amenable to resection may not be candidates for general anesthesia, may have hepatic dysfunction precluding resection, or may refuse surgical intervention. Therefore, minimally invasive treatment of hepatic tumors has become an area of considerable interest [9, 10].

Radiofrequency (RF) ablation is an interstitial focal ablative therapy in which an electrode is placed into a liver lesion to cause tissue heating from ionic agitation, resulting in heating and cauterization of the tumor mass and probe track. Unlike cryoablation, RF probes are of smaller diameter (generally 15–18 gauge) and can be used in a percutaneous fashion, with minimal risk of bleeding [11, 12]. To date, guidance for RF ablation in clinical series has been almost exclusively

Received November 18, 1999; accepted after revision January 28, 2000.

Supported in part by RITA, Mountain View, CA.

<sup>1</sup>Department of Surgery, University of Wisconsin, 600 Highland Ave., Madison, WI 53792-3252.

<sup>2</sup>Department of Radiology, University of Wisconsin, Madison, WI 53792-3252. Address correspondence to F. T. Lee, Jr.

<sup>3</sup>Department of Pathology, University of Wisconsin, Madison, WI 53793-3252.

AJR 2000;175:705–711

0361–803X/00/1753–705

© American Roentgen Ray Society

through the use of conventional transabdominal sonography [12, 13]. Advantages of using sonographic guidance for RF ablation include widespread availability, real-time guidance for probe placement, and accurate and convenient puncture guides available for most probe systems. However, local recurrence rates as high as 34–54.5% have been reported for percutaneous RF ablation guided by conventional sonography [12–14]. This is a rate much higher than the 12% local recurrence rate reported for cryosurgical patients followed for at least 5 years [15] or the less than 16.7% local recurrence rate reported for surgical resection [16].

One of the critical factors contributing to the success of cryoablation of liver tumors has been the superb imaging of liver tumors and the iceball with intraoperative sonography. Because of the marked refraction and reflection of the sonographic beam at the interface between frozen and unfrozen liver, the iceball is readily apparent on intraoperative sonography [17, 18]. In contrast, the zone of necrosis during RF ablation is not easily visualized by transabdominal sonography as a result of low intrinsic contrast between normal and ablated liver and artifacts from gas bubble formation and the RF generator. These conditions result in uncertainty in determining the extent of ablation during an RF procedure and may be a contributing factor to the high positive margin rates seen in clinical series [12, 13]. The purpose of this study is to determine whether it is possible to improve visualization of RF ablative lesions through the use of CT during the procedure and whether CT has advantages over sonography for this purpose.

## Subjects and Methods

### *Animals and Anesthesia*

Approval for this protocol was obtained through the University of Wisconsin Research Animal Resource Committee. Four female pigs (mean weight, 23 kg) who otherwise had access to food and water ad libitum were fasted for 12 hr before the study. General anesthesia was induced with an intramuscular injection of tiletamine and zolazepam (Telazol; Fort Dodge Laboratories, Fort Dodge, IA) and xylazine (Rompun; Bayer, Shawnee Mission, KS). Anesthesia was maintained with inhaled isoflurane 1–3%. A dispersive grounding pad was applied to the animal's flank before surgery after shaving body hair. The abdomen was also shaved to decrease interference with sonography.

### *RF Ablation*

Fifteen-gauge RF probes (Model 30; RITA Medical Systems, Mountain View, CA) with four retractable electrodes deployable to a maximum diameter of 3 cm were used for all RF ablation de-

scribed in this study. Each of the four prongs is equipped with a thermosensor at the tip, and the probe is insulated to within 1 cm of the tip. The RF generator (RITA Medical Systems) delivers a 460-kHz continuous unmodulated sinusoidal waveform in the bipolar output mode.

Four RF ablative lesions were created in each of three pigs for a total of 12 lesions. A portion of the pig liver was chosen for probe placement with sonographic guidance. Probes were placed percutaneously into the liver in separate areas using a freehand technique. Tissue ablation was performed for 13 min at approximately 95°C as measured by the thermosensors arrayed at the tip of each tine.

A single additional pig was used to obtain timed specimens for histologic study without imaging. This animal was anesthetized as described previously, and open laparotomy was performed through a bilateral subcostal incision. An RF probe was placed into the liver parenchyma and 2-, 8-, and 13-min ablations were performed in separate locations. After each treatment, the liver lesion was immediately resected and preserved in formalin. The animal was sacrificed as described in the following text.

### *CT and Sonographic Monitoring*

Lesions were imaged with both CT and sonography before ablation and at 2 min, 8 min, and immediately after ablation. The experiment was designed using a crossover technique in which the order of scanning alternated for each lesion. This system resulted in six lesions in which CT was performed first and six lesions in which sonography was first. All CT was performed on a CTi helical scanner (General Electric Medical Systems, Milwaukee, WI). Helical CT was performed at each time point and encompassed the RF probe tip and ablation zone using collimation of 3 mm and a pitch of 1:1. After completion of the last burn in each pig, contrast-enhanced CT was performed using 2 mL/kg of iohexol 300 injected at 2 mL/sec.

All sonograms were obtained using 128-XP scanner (Acuson, Mountain View, CA) using a curved array 5-MHz transducer. Sonography was performed corresponding to the unenhanced CT with the CT laser guide to reproduce the same axial plane and scanning level. If an anterior view did not yield a sufficiently clear acoustic window, any site along the identical axial plane (as defined by the CT laser light) was considered sufficient if the probe tip could be visualized. Once an appropriate acoustic window was achieved, it was held constant throughout the ablation. Images were recorded and archived digitally (UltraPACS version 3.1; ALL, Richmond, B.C., Canada).

### *Tissue Harvest*

After RF ablation, pigs were returned to their cages for 24–48 hr and reanesthetized. A bilateral subcostal incision was performed for liver exposure and the portal vein was cannulated. Heparin (4000 IU) was administered IV, and the animals were sacrificed with an IV overdose of beuthanasia-d (Euthasol [390 mg pentobarbital sodium, 50 mg phenytoin sodium];

Schering-Plough, Kenilworth, NJ). The suprahepatic inferior vena cava was ligated and 1.0 L of 10% neutral buffered formalin was infused into the portal vein. The liver was then removed en bloc and immersed in formalin. Livers were allowed to fix for 1 week and were sliced in the axial plane approximating the CT slice planes at 5-mm intervals. The RF lesions grossly consisted of an outer red zone and an inner pale zone. The inner pale zone was used for lesion measurements in two planes.

### *Histopathology*

Analysis of the RF lesions was performed with both standard histology and electron microscopy. Tissue fixed in neutral buffered formaldehyde was paraffin-embedded and stained with H and E. A 10× ocular micrometer was used for measurements of cell plates. Tissue blocks for ultrastructural examination were fixed in 2.5% phosphate-buffered glutaraldehyde, postfixed in osmium tetroxide, dehydrated in graded ethanols and propylene oxide, and then infiltrated in EM bed 812 (Eketron Microscopy Sciences, Fort Washington, PA). Ultrathin sections were stained with lead citrate and uranyl acetate. Thick Epon sections were stained with toluidine blue.

### *Data Collection and Statistics*

Representative images from each ablation were coded with a random number generator and all identifying material deleted from the film. Three radiologists experienced in both CT and sonography and blinded to the details of the tissue ablation evaluated RF lesions on sonography and CT with regard to the following: differentiation from background liver, visualization of the liver and lesion interface, and the presence of artifacts that affected the ability to visualize the lesion. Data were ranked on a scale of 1–5 (1 = no visible differentiation between liver and lesion, 2 = visible but with low confidence, 3 = visible with moderate confidence, 4 = visible with high confidence, 5 = extraordinarily visible). Overall attenuation and echogenicity of the RF lesion were also evaluated by the reviewers.

RF lesion measurements at imaging were obtained on the slice with the largest transverse diameter. Two dimensions for each lesion (the greatest diameter and an orthogonal diameter) were averaged to obtain a mean dimension. Lesions seen on CT were measured with calipers and an internal size standard. All sonographic measurements were performed with a commercially available measuring package on the mini-PACS (mini-picture archiving and communication system) unit. Note that for lesion measurements, only postablation images were used for comparison with pathology. For pathologic correlation, direct measurements of RF lesions in liver sections were obtained from the section best corresponding to the imaging plane. For Hounsfield-unit values before ablation and at each time point, three representative values of the RF lesion were obtained and averaged in the area most devoid of artifacts. In addition, three values of normal liver

## Imaging in Liver Ablation

parenchyma in an area devoid of both artifacts and vessels were obtained and a mean value was obtained. The largest region of interest consistent with uniformity of the sample was used.

Blinded observer rankings were compared with a nonparametric assumption for paired data (Wilcoxon's signed rank test). Hounsfield-unit data from the same lesion over time were compared with a

paired Student's *t* test, and comparisons between different lesions used an unpaired Student's *t* test. Lesion sizes on various imaging techniques versus pathology were compared using simple regression.

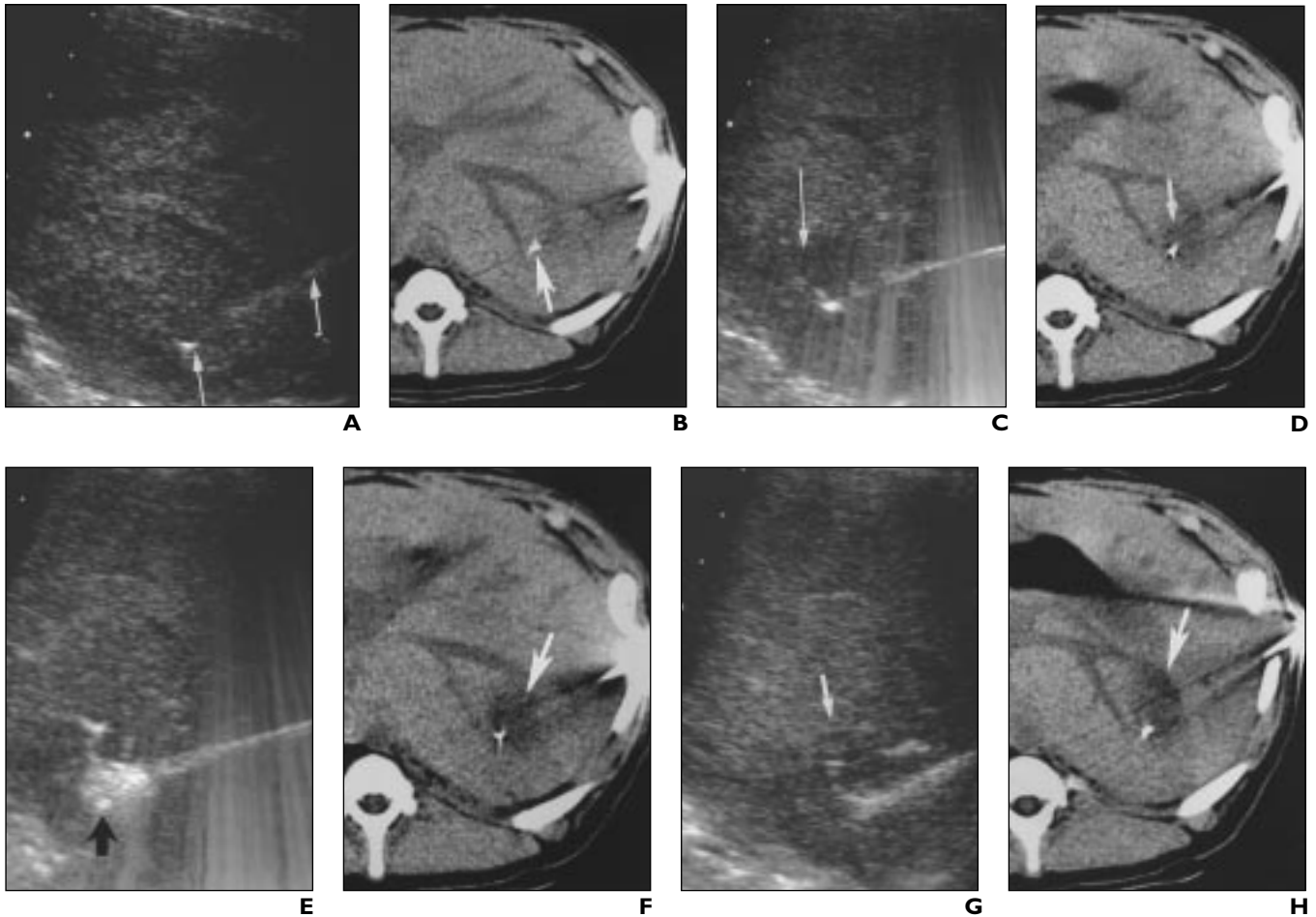


**Fig. 1.**—CT and sonographic imaging of radiofrequency (RF) ablation in female pigs over time.

**A,** Sonogram before ablation shows RF probe (*arrows*) in place.

**B,** Unenhanced CT scan before ablation at same level as **A** shows RF probe in place (*arrow*).

**C,** Sonogram obtained 2 min after start of ablation shows slightly hypoechoic RF lesion (*arrow*).

**D,** Unenhanced CT scan obtained 2 min after start of ablation shows hypoattenuating RF lesion (*arrow*) similar to that seen in **C**.

**E,** Sonogram 8 min into ablation shows presence of hyperechoic material (*arrow*) probably representing gas in central RF lesion.

**F,** Unenhanced CT scan 8 min into ablation shows that RF lesion is well demarcated (*arrow*).

**G,** Sonogram immediately after ablation shows that hyperechoic material is no longer apparent in center of lesion. Poorly defined hypoechoic zone of ablation remains (*arrow*).

**H,** Unenhanced CT scan immediately after ablation shows that lesion (*arrow*) has not appreciably changed from 8-min image.

**I,** Contrast-enhanced CT scan after ablation shows central portion of lesion as well defined and correlating with liver section. Nonenhancing area (*arrows*) in contact with capsule is caused by interruption of blood supply peripheral to RF lesion rather than ablated area. In this case, contrast-enhanced CT overestimates zone of ablation.

**J,** Gross liver section at same level as CT scans and sonograms shows normal liver tissue peripheral to RF lesion (*arrows*). Additional peripheral lesion (*asterisk*) was from separate ablation. Area in central lesion (*white square*) is from hemorrhage into area of complete ablation.

**Results**

During imaging, all RF ablations were monitored with CT and sonographic guidance. On sonography, finding an acoustic window was not difficult, and the needle shaft and prongs were easily visualized in all cases. All animals survived to complete the entire protocol, and no complications were detected at either imaging or sacrifice. Specifically, no evidence of bleeding from any hepatic puncture site was found.

*Blinded Observer Analysis*

The relative scores for conspicuity of lesions, border discrimination, and the presence of artifacts are shown in Table 1. Unenhanced CT significantly improved observer visualization of RF lesions compared with sonography ( $p < 0.05$ ). Border discrimination between liver and lesion was improved using unenhanced CT ( $p < 0.05$ ). Unenhanced CT also decreased the amount of artifacts as compared with sonography ( $p < 0.05$ ). Contrast-enhanced CT further increased the ability of the blinded observers to discriminate lesion from liver and to define the

lesion borders and appeared to decrease the impact of artifacts on defining the RF lesion ( $p < 0.05$ ) (Fig. 1). Of note, unenhanced CT was performed throughout the RF ablative process, whereas contrast-enhanced CT was performed only after ablation.

The RF lesion had consistently lower attenuation values than surrounding normal liver at all time points ( $p < 0.05$ ) (Table 2). The attenuation difference between liver and lesion was most marked at 8 min (22.2 H,  $p <$

0.05). Low-attenuation values relative to normal liver were seen in areas both with and without detectable gas bubbles on CT. As expected, no difference in attenuation before initiation of ablation ( $p = 0.28$ ) was found. After ablation and after contrast enhancement, an increase in attenuation of both normal liver and RF lesions was seen. The increase in lesion attenuation after contrast material administration was disproportionately low when compared with normal liver,

<b>TABLE 1 Results: Masked Observers Unaware of Treatment Status</b>			
Category	Mean Rank		
	Obtained During and Immediately After Ablation		Contrast-Enhanced CT Scans Obtained After Ablation <sup>b</sup>
	Sonograms	Unenhanced CT	
Lesion vs. liver	2.2	2.8	4.3
Border discrimination	2.0	2.4 <sup>b</sup>	4.1
Presence of artifact <sup>a</sup>	2.9	3.2 <sup>b</sup>	4.9

Note.—Three radiologists evaluated radiofrequency lesions on sonography and CT.

<sup>a</sup>Measured on a scale of 1–5 (1 = severe artifacts, 5 = no artifacts).

<sup>b</sup> $p < 0.05$  compared with sonography on Wilcoxon's signed rank test.

<b>TABLE 2 Attenuation Values of Radiofrequency (RF) Lesions (H)</b>					
Imaging	Lesions	RF Lesion	Normal Liver	Liver vs. Lesion Difference	$p^a$ (Liver vs. Lesion)
Baseline	12	49.8	51.0	1.2	0.28
Unenhanced CT					
2 min	12	37.8	51.5	13.7	0.0001
8 min	12	29.6	51.8	22.2	<0.0001
After ablation					
Unenhanced CT	12	34.0	50.2	16.2	<0.0001
Contrast-enhanced CT	12	49.8	104.3	54.5	<0.0001

<sup>a</sup> Student's paired *t* test.

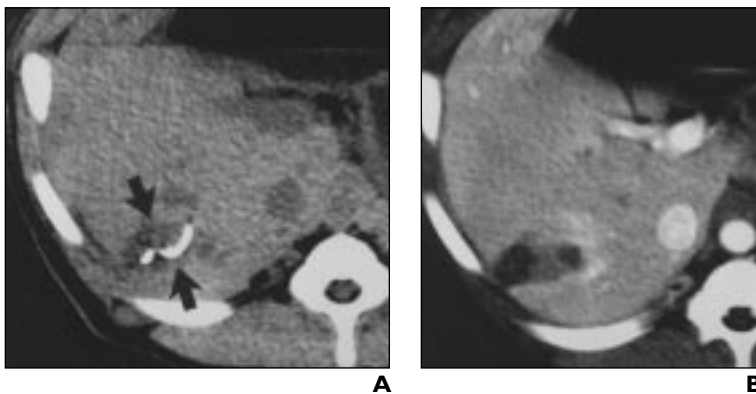


**Fig. 2.**—Increased visibility of CT lesions with contrast enhancement in female pigs. **A**, Unenhanced CT scan after ablation shows that hypoattenuating ablation zone (arrows) is moderately apparent surrounding prongs of radiofrequency probe. **B**, Contrast-enhanced CT scan shows that lesion is much more visible primarily because of increase in attenuation of background liver.

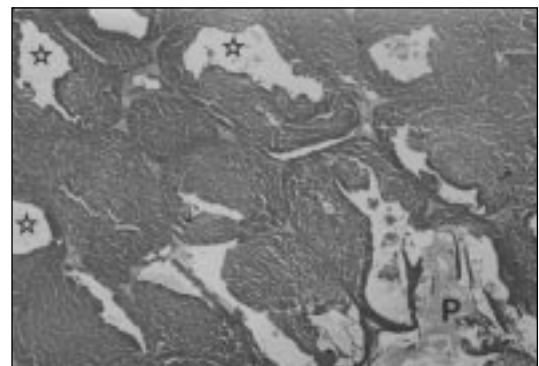


**Fig. 3.**—Photomicrograph of histopathologic specimen shows gas bubble in hepatic parenchyma (stars) with microfissures in lobules. Site of prong (P) shows rupture and dense compression of liver. (H and E,  $\times 20$ )

## Imaging in Liver Ablation

leading to a marked increase in the liver-lesion attenuation difference (Fig. 2).

Most RF lesions were hypoattenuating on CT and hypoechoic on sonography (hypoechoic = 59%, hyperechoic = 25%, isoechoic = 16%). Occasionally, the same lesion was seen to change echogenicity over time (Fig. 1). RF lesions on CT were more uniformly hypoattenuating. The minority of lesions that were graded as hyperattenuating by the blinded observers were likely caused by streak artifacts passing through and obscuring the RF lesion.

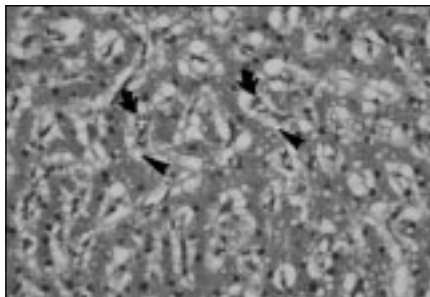


**Fig. 4.**—Photomicrograph of histopathologic specimen shows separation of sinusoidal vessels (curved arrows) from shrunken liver cell plates (arrowheads) that contain small vacuoles. (H and E,  $\times 200$ )

### Histopathology and Electron Microscopy

Examination of RF lesions in the outer red zone (1- to 5-mm thickness) showed hemorrhage, congestion, and partial necrosis of hepatocytes. Some viable cells were identified in this zone. The inner pale zone showed compressed hepatocytes in the vicinity of clusters of gas bubbles (Fig. 3). Peripheral to the area of compression, a zone of pallor was caused by shrinkage of hepatocytes and separation from sinusoidal endothelium (Fig. 4). The cytoplasm of hepatocytes was more eosinophilic than nor-

mal, nuclei were smaller, and chromatin was condensed. Ultrastructural (electron microscopic) examination of a lesion at 8 min showed outlines of hepatocyte nuclei with prominent nucleoli in pale granular chromatin. Ribosomes were aggregated and rough endoplasmic reticulum was destroyed. Outlines of cell walls were barely perceptible and the periphery of hepatocytes was ragged. The sinusoids contained ruptured compressed erythrocytes. In some veins, amorphous erythrocyte debris was compressed against the vessel wall by a central bubble of gas (Fig. 5). No evidence of viable hepatocytes in the pale zone was seen by electron or light microscopy. Pathologic changes seen at the light microscopic level in the zone of damage did not change over time.

### RF Lesion Size: Imaging Versus Pathology

The results of imaging compared with actual size of lesions seen on gross pathologic examination are shown in Table 3. Unenhanced CT had the best correlation to pathologic size ( $r = 0.74$ ), even better than contrast-enhanced CT ( $r = 0.72$ ), which slightly overestimated lesion size (Figs. 1H and 1I). However, with the exception of the overestimation of lesion size as a result of ischemia peripheral to the RF lesion, contrast-enhanced CT subjectively corresponded the most closely of any imaging technique with lesion shape. Sonography had the poorest correlation to lesion size ( $r = 0.56$ ).

Imaging	Mean Size (cm)	Correlation with Pathology	
		$r^a$	$r2^b$
		Unenhanced CT	2.70 $\pm$ 0.8
Contrast-enhanced CT	3.10 $\pm$ 1.0	0.72	0.52
Sonography	2.5 $\pm$ 0.7	0.56	0.31
Pathology	3.03 $\pm$ 0.9	NA	NA

<sup>a</sup>Correlation coefficient.

<sup>b</sup>Coefficient of determination.

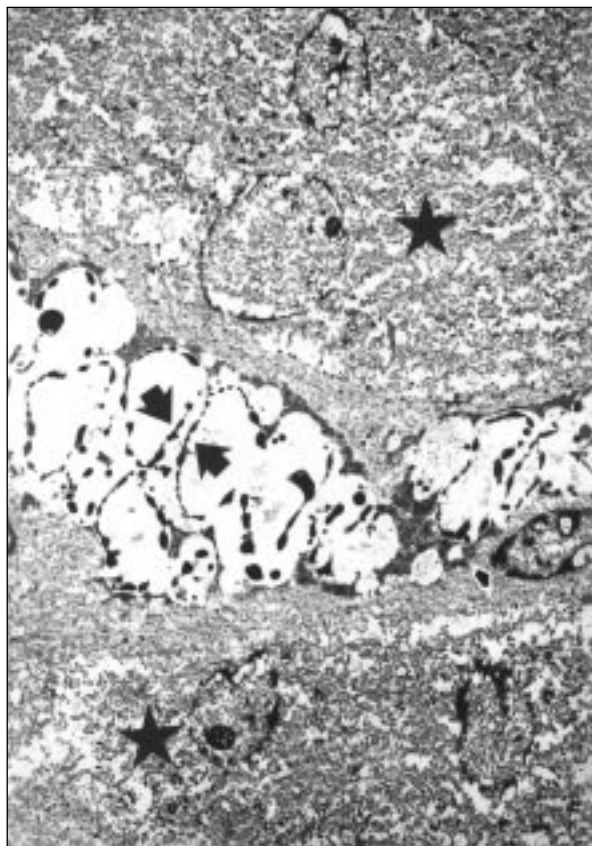


**Fig. 5.**—Ultrastructural (electron microscopic) appearance of liver shows beaded outlines of erythrocytes (large arrows) in remnant of sinusoid and nucleus of endothelial cell (small arrow). Note outlines of liver cell plates on both sides of sinusoid (stars). ( $\times 3600$ ).

### Discussion

Percutaneous RF thermal ablation is a promising technique for treating hepatic tumors but has been limited by a high local recurrence rate [12–14]. Two explanations for recurrences after RF ablation are possible. The first is that the RF lesion inadequately covered the tumor. The second explanation is that the tumor was adequately covered but that the application of RF energy did not kill the entire tumor. We believe that most local recurrences after RF are the result of inadequate initial tumor ablation, with residual viable tumor remaining at portions of the peripheral margin. This residual tumor often recurs in a circular fashion around the original tumor and is difficult to treat with a follow-up application of RF [12]. Therefore, initial precise determination of the adequacy of ablation margins can be expected to decrease the local recurrence rate.

Typically, RF ablation is monitored using real-time transabdominal sonography, followed by CT or MR imaging some time after

the procedure. Sonography has the advantage of being readily and widely available, is an excellent real-time imaging technique for probe placement, and is a reasonably good technique for visualizing hepatic tumors. However, during the ablation, artifacts created by thermal tissue changes and the low contrast resolution of sonography limit the ability of sonography to precisely visualize the extent of necrosis [12, 13]. Hyperechoic areas in the liver from gas formation are created during the application of RF energy, but these foci do not closely correspond to areas of tissue necrosis [12]. These limitations can severely hinder the ability to accurately determine the area of ablation during the procedure, leading to overtreatment of some previously ablated areas and undertreatment of others. We believe that the lack of concordance between imaging findings during the procedure and tissue ablation is responsible for many of the local tumor recurrences after RF therapy. In this study, sonography was "fixed" to the axial imaging plane. This limitation was necessary because of the critical need for precise pathologic correlation. In the pigs used for this study (unlike many humans), the acoustic windows were more than sufficient to localize the RF probe and monitor the ablation. In fact, the ablations in this study were more easily monitored with the use of a 5-MHz sonographic transducer than ablations in our human patients, and thus we do not believe the difference between porcine and human sonography was an important source of bias.

A marked discrepancy has been reported between the rate of local recurrences for percutaneous RF [12–14] versus intraoperative [10] cases. The reasons for this are probably multifactorial but include the vascular occlusion associated with operative cases and precise monitoring of probe placement (and possibly lesion formation) by intraoperative sonography [19]. The efficacy of conventional sonography may be increased when used in conjunction with color Doppler sonography and sonographic contrast agents [20].

The use of intraprocedural CT to monitor RF ablation has not been extensively explored in the literature. Several potential clinical advantages of CT for this purpose include the following: confirmation of probe placement in relation to the tumor, improved visualization of the extent of ablation with respect to fixed anatomic landmarks, and correlation to preablation scans to increase confidence of complete tumor ablation. CT scanners are also readily available, and radi-

ologists are comfortable with placement of needles into liver masses with CT guidance. It is debatable whether liver lesions are better seen on unenhanced CT or sonography, but if uncertainty exists over lesion location during the RF ablation, a small bolus of contrast material can be given and the area scanned during the procedure.

This study shows several additional advantages of CT when compared with sonography for the monitoring of RF ablation. RF lesions and liver-lesion interfaces were better visualized with CT than sonography. Distinguishing this interface is especially important because it determines the duration and extent of ablation. An ideal ablation would encompass the tumor plus a 1-cm margin of normal liver. Surgical margins of at least 1 cm at hepatic resection have been shown to increase long-term survival [16]. In the absence of any data to the contrary, it is a reasonable assumption that ablative therapies should strive for a similar margin.

An additional advantage of CT over sonography in this study was better correlation with proven lesion size at pathology. Of the three techniques (unenhanced CT, contrast-enhanced CT, and sonography), unenhanced CT had the closest correlation with actual lesion size, whereas sonography tended to underestimate lesion size. Several explanations for this finding are possible: low intrinsic contrast between liver and RF lesion by sonography can increase uncertainty concerning liver and lesion borders; artifacts appeared to be more troublesome on sonography when evaluating lesion size. One explanation may be the fixed anatomic landmarks available on CT, and slight differences in imaging plane on sonography can substantially change the size of the measured ablative zone [21]. An interesting additional finding was that contrast-enhanced CT tended to slightly overestimate ablative-zone size (Fig. 1I). We have seen this phenomenon in CT after cryoablation and believe that it is caused by relative obstruction of blood flow in areas peripheral to the ablation. Because both the ablative zone and peripheral liver are unenhanced, separating the border between the ablative zone and unperfused liver can be difficult.

Despite the advantages of CT elucidated in this study, several inherent limitations may cause difficulty during clinical cases. The most obvious is the increased time that will be necessary for probe placement with CT as compared with sonography: most CT scanners do not have real-time capability. Unlike percutaneous biopsy, in which any part of a liver mass may be sampled, ablative therapies are highly dependent on precise probe positioning if complete

tumor ablation is the goal. Therefore, multiple probe repositionings can be anticipated before tumor ablation. Most tumors will require several ablations for complete coverage, leading to a procedure that may last several hours overall. This limitation may be obviated by the advent of real-time or fluoroscopic CT should it become more widely available [22]. We have also combined the use of sonography and CT for clinical cases. Sonography can be used to guide probe placement, and CT, for monitoring the extent of ablation.

Other limitations to the use of CT for RF ablation include the fixed imaging in the axial plane. This can lead to difficulty ablating tumors under the diaphragm or in other areas where oblique imaging planes are desirable. In addition, the use of CT exposes both the patient and physician to ionizing radiation, particularly when multiple probe repositionings and ablations are anticipated. Recently, MR imaging has also been investigated in the monitoring of hepatic RF ablation. Though some success has been seen with MR imaging-guided RF, it has been limited by extensive artifacts [23]. MR imaging is also expensive, cumbersome, and requires specialized interventional MR imaging units and MR imaging-compatible RF units that will seriously impede the widespread use of MR imaging for RF regardless of potential advantages [24]. However, because of the excellent contrast resolution provided by MR imaging, we expect that MR imaging-guided RF will prove useful when the technical limitations have been overcome.

In summary, this study shows that CT can more accurately monitor RF thermal ablation than transabdominal sonography in this animal model. CT was better at identifying lesion sizes and lesion borders and was less limited by artifacts. The use of CT may reduce the high rate of local recurrence associated with percutaneous RF ablation, a technique with otherwise minimal morbidity and great potential in the treatment of malignant hepatic disease.

#### Acknowledgments

We thank Karen Schorr and Kim Echeimer for their help with sonography and tissue preparation, Carrie Poole for manuscript preparation, and Alan H. Rappe and Margaret Rankin for animal assistance. We also thank our blinded observers for the tedious chore of film interpretation.

#### References

1. Bridbord K. Pathogenesis and prevention of hepatocellular carcinoma. *Cancer Detect Prev* 1989;14:191–192

## Imaging in Liver Ablation

2. Steele G Jr. Colorectal cancer metastatic to the liver: resection. In: Cameron JL, ed. *Current surgical therapy*, 5th ed. St. Louis: Mosby, **1995**:283–289
3. Ringe B, Pichlmayr R, Wittekind C, Tusch G. Surgical treatment of hepatocellular carcinoma: experience with liver resection and transplantation in 198 patients. *World J Surg* **1991**;15:270–285
4. Nagorney DM, Gigot JM. Primary epithelial hepatic malignancies: etiology, epidemiology, and outcome after subtotal and total hepatic resection. *Surg Oncol Clin N Am* **1996**;5:283–300
5. Zhou XD, Tang YU, Yu YQ, et al. The role of hepatic cryosurgery in the treatment of hepatic cancer: a report of 113 cases. *J Cancer Res Clin Oncol* **1993**;120:100–102
6. Weaver ML, Ashton JG, Zemel R. Treatment of colorectal metastases by cryotherapy. *Semin Surg Oncol* **1998**;14:163–170
7. Hghes KS, Simon R, Songharabodi S, et al. Resection of the liver for colorectal carcinoma metastases: a multi-institutional study of indications for resection. *Surgery* **1988**;103:278–288
8. Korpan NN. Hepatic cryosurgery for liver metastases: long-term follow-up. *Ann Surg* **1997**;225:193–201
9. Lee FT Jr, Chosy SG, Weber SM, Littrup PJ, Warner TF, Mahvi DM. Hepatic cryosurgery via minilaparotomy in a porcine model: an alternative to open cryosurgery. *Surg Endosc* **1999**;13:253–259
10. Curley SA, Izzo F, Delrio P, et al. Radiofrequency ablation of unresectable primary and metastatic hepatic malignancies: results in 123 patients. *Ann Surg* **1999**;230:1–8
11. Curley SA, Davidson BS, Fleming RY, et al. Laparoscopically guided bipolar radiofrequency ablation of areas of porcine liver. *Surg Endosc* **1997**;11:729–733
12. Solbiati L, Goldberg SN, Ierace T, et al. Hepatic metastases: percutaneous radio-frequency ablation with cooled-tip electrodes. *Radiology* **1997**;205:367–373
13. Solbiati L, Ierace T, Goldberg SN, et al. Percutaneous US-guided radio-frequency tissue ablation of liver metastases: treatment and follow-up in 16 patients. *Radiology* **1997**;202:195–203
14. Rossi S, Di Stasi M, Buscarini E, et al. Percutaneous RF interstitial thermal ablation in the treatment of hepatic cancer. *AJR* **1996**;167:759–768
15. Kane RA, McPhee DM, Kruskal JB, Jenkins RL, Lewis WD, Cady B. Five year survival in US-guided hepatic cryosurgery (abstr). *Radiology* **1997**;205:201
16. Hghes K, Scheele J, Sugarbaker PH. Surgery for colorectal cancer metastatic to the liver: optimizing the results of treatment. *Surg Clin North Am* **1989**;69:339–359
17. Lee FT Jr, Mahvi DM, Chosy SG, et al. Hepatic cryosurgery with intraoperative US guidance. *Radiology* **1997**;202:624–632
18. Ravikummar TS, Steele G Jr, Kane R, King V. Experimental and clinical observations on hepatic cryosurgery for colorectal metastases. *Cancer Res* **1991**;51:6323–6327
19. Mahvi DM, Lee FT Jr. Radiofrequency ablation of hepatic metastases: is heat better than cold? *Ann Surg* **1999**;230:9–11
20. Solbiati L, Goldberg SN, Ierace T, Dellanoce M, Liverish T, Gazelle GS. Radio-frequency ablation of hepatic metastases: post-procedural assessment with a US microbubble contrast agent—early experience. *Radiology* **1999**;211:643–649
21. Littrup PJ, Williams CR, Egglin TK, Kane RA. Determination of prostate volume with transrectal US for cancer screening. II. Accuracy of in vitro and in vivo techniques. *Radiology* **1991**;179:49–53
22. Daly B, Templeton PA. Real-time CT fluoroscopy: evaluation of an interventional tool. *Radiology* **1999**;211:309–315
23. Boaz TL, Lewin JS, Chung YC, Duerk JL, Clampitt ME, Haaga JR. MR monitoring of MR-guided radiofrequency thermal ablation of normal liver in an animal model. *J Magn Reson Imaging* **1998**;8:64–69
24. Lewin JS, Connell CF, Duerk JL, et al. Interactive MRI-guided radiofrequency interstitial ablation of abdominal tumors: clinical trial for evaluation of safety and feasibility. *J Magn Reson Imaging* **1998**;8:40–47